

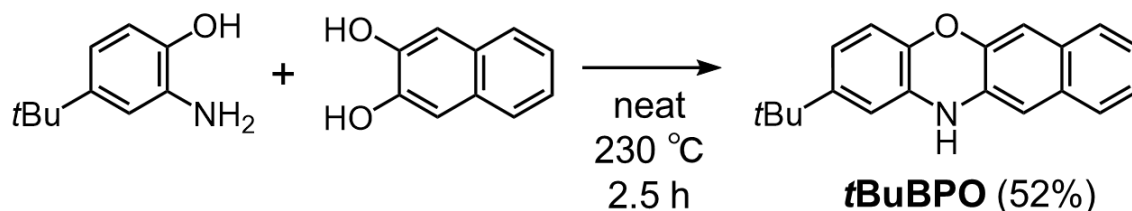
Contents

p.S2	General Information
p.S3–S5	Synthetic Details
p.S6–S8	NMR Spectra
p.S9–S12	X-ray Crystal Structure Analyses
p.S13–S14	DFT Calculations
p.S15–S16	Emission Lifetime Measurement
p.S17–S21	Optical Resolution of 2
p.S22–S24	Optimized geometries of 2

General Information

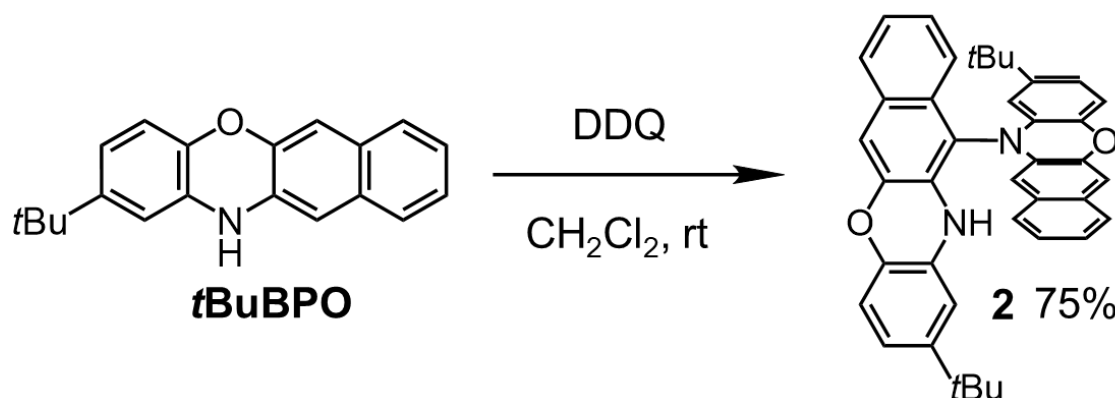
All the purchased reagents were of standard quality and used without further purification. All the mechanochemical reactions were carried out under air. Mechanochemical reactions were performed using a Retsch MM400 mixer mill. Flash chromatography was performed with a Biotage Isorela medium pressure liquid chromatography (MPLC) system and a SNAP Sfar flash silica gel cartridge (Biotage). ^1H and ^{13}C NMR spectra were recorded by a Varian 400-MR FT-NMR spectrometer. Matrix-assisted laser desorption ionization TOF mass spectra were obtained on a Shimadzu MALDI-8020 mass spectrometer. UV-vis-NIR absorption spectra were obtained with a JASCO V-670 spectrometer. Emission spectra were measured with a Shimadzu RF-6000 spectrofluorometer. Emission quantum yields were measured using an integrating sphere. Cyclic voltammetry and differential pulse voltammetry were measured in BAS Electrochemical Analyzer ALS Model 612B. Circular dichroism (CD) spectra were recorded on a JASCO J-820 spectropolarimeter with CH_2Cl_2 as a solvent at room temperature. Circularly polarized luminescence (CPL) spectra were recorded on a JASCO CPL-200S. Variable-temperature emission and CPL spectra were measured using a UNISOKU CoolSpeK cryostat.

Synthetic Details



tBuBPO: 2-amino-4-*tert*-butylphenol (2.48 g, 15.0 mmol) and 2,3-dihydroxynaphthalene (2.40 g, 15.0 mmol) were ground together with a mortar and pestle. The mixed solid was placed in a round-bottom flask and heated under N₂ atmosphere at 230 °C for 150 min. After cooling to r.t., the resulted sold was washed with Et₂O. By drying the solid under reduced pressure, **tBuBPO** was obtained as a gray powder (2.23 g, 7.78 mmol, 52%). ¹H-NMR (400 MHz, CD₂Cl₂) δ 7.50 (q, *J* = 8.2 Hz, 2H), 7.25–7.17 (m, 2H), 7.02 (s, 1H), 6.75–6.69 (m, 3H), 6.56 (s, 1H), 5.76 (s, 1H), 1.27 (s, 9H). ¹³C-NMR could not be recorded because of its low solubility. MALDI-TOF MASS (Matrix = dithranol) (C₂₀H₁₉NO): Found = 289.1; Calcd. 289.1467

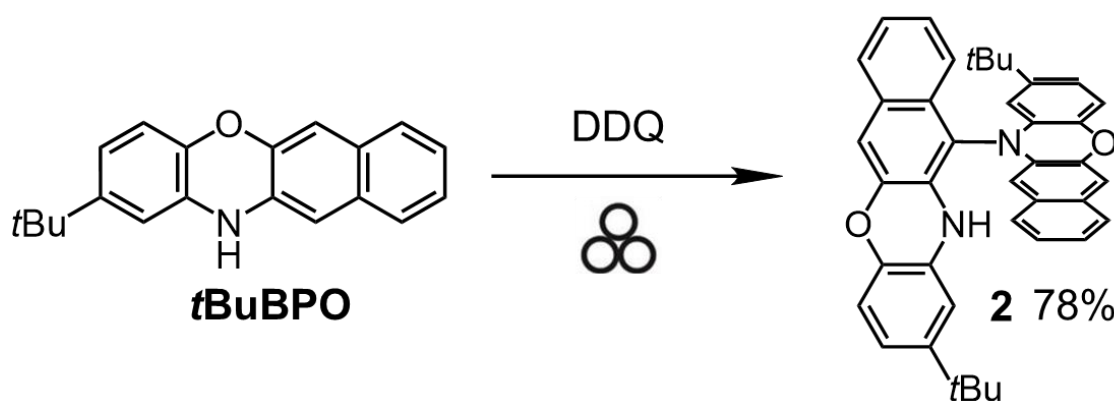
Synthesis of **2** via solution-phase reaction



2 (solution-phase reaction) : **tBuBPO** (579 mg, 2.00 mmol) was dissolved in 100 mL of

dichloromethane and stirred at room temperature under N₂ atmosphere. To the solution, DDQ (341 mg, 1.50 mmol) was added and the solution was stirred at room temperature for 1 h. The reaction mixture was quenched by adding small amount of hydrazine hydrate and filtered through celite. The crude solution was washed with water and the organic layer was dried over Na₂SO₄. After removing the solvent under reduced pressure, the crude product was chromatographed on silica gel (ethyl acetate/hexane as eluent) to afford **2** (418 mg, 73%) as a pale-yellow powder. ¹H-NMR (400 MHz, CD₂Cl₂) δ 7.59–7.37 (m, 2H), 7.16–7.03 (m, 7H), 6.75–6.65 (m, 4H), 6.45 (s, 1H), 6.20–6.00 (m, 3H), 1.08 (s, 9H), 0.91 (s, 9H). ¹³C-NMR (100 MHz, CD₂Cl₂) δ 31.19, 31.34, 34.42, 34.54, 108.44, 111.22, 111.54, 1112.01, 1112.03, 112.48, 115.33, 115.56, 118.93, 119.02, 121.78, 124.65, 124.78, 125.37, 126.25, 126.53, 126.60, 127.95, 128.10, 128.41, 130.27, 130.71, 130.88, 131.29, 131.80, 131.88, 140.72, 141.64, 144.78, 144.97, 147.48, 147.61. MALDI-TOF MASS (Matrix = dithranol) (C₄₀H₃₆N₂O₂): Found = 576.2; Calcd. 576.2777.

Synthesis of **2** via mechanochemical reaction



In a 50 mL stainless-steel jar of a mixer mill, **tBuBPO** (500 mg, 1.73 mmol) and DDQ (236 mg, 0.6 eq.) were placed with twelve stainless steel balls (10 mm φ) and milled at 30 Hz for 30 min. After milling, the reaction mixture was extracted with CH₂Cl₂ and

quenched by adding hydrazine hydrate (2 mL). The reaction solution was filtered through celite and the filtrate was washed with water. The organic layer was dried over Na₂SO₄, and the solvent was removed under reduced pressure. The crude product was chromatographed on silica gel (ethyl acetate/hexane as eluent) to afford **2** (389 mg, 78%) as a yellow powder.

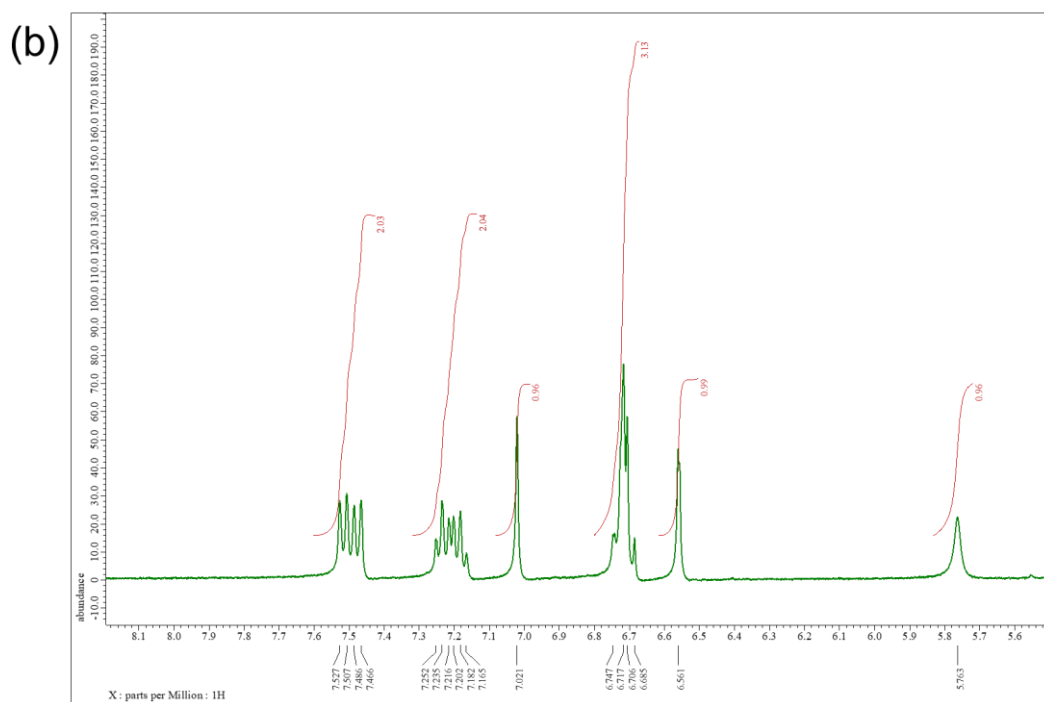
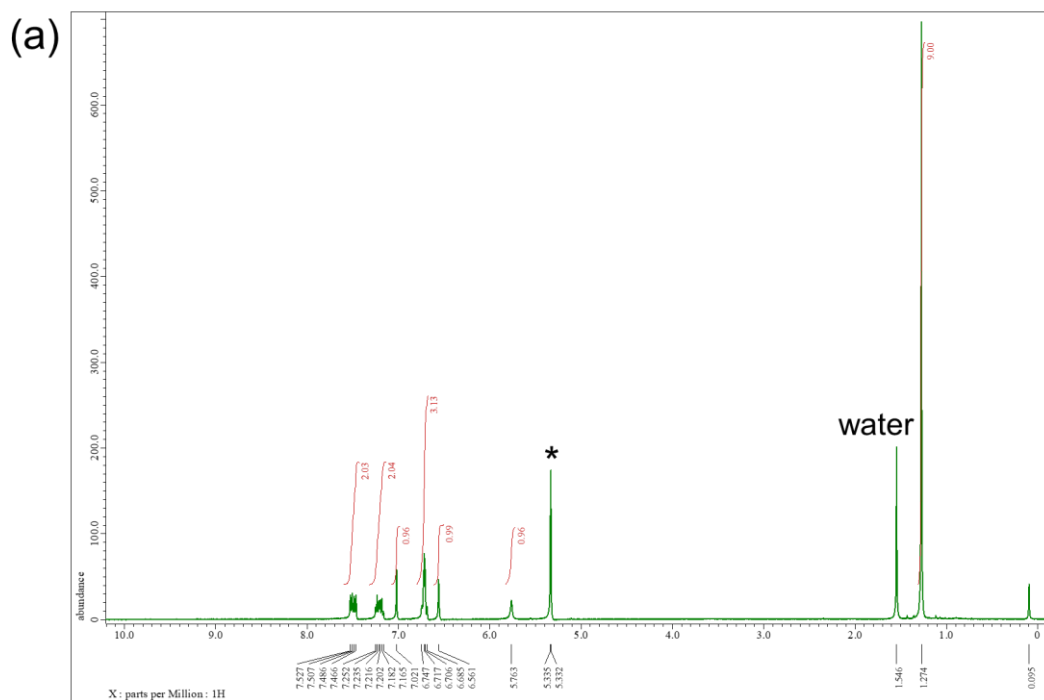


Fig. S1 ^1H NMR spectra of **tBuBPO** in dichloromethane- d_2 . a) 0–10 ppm and b) aromatic region. Asterisk denotes the solvent residual peak.

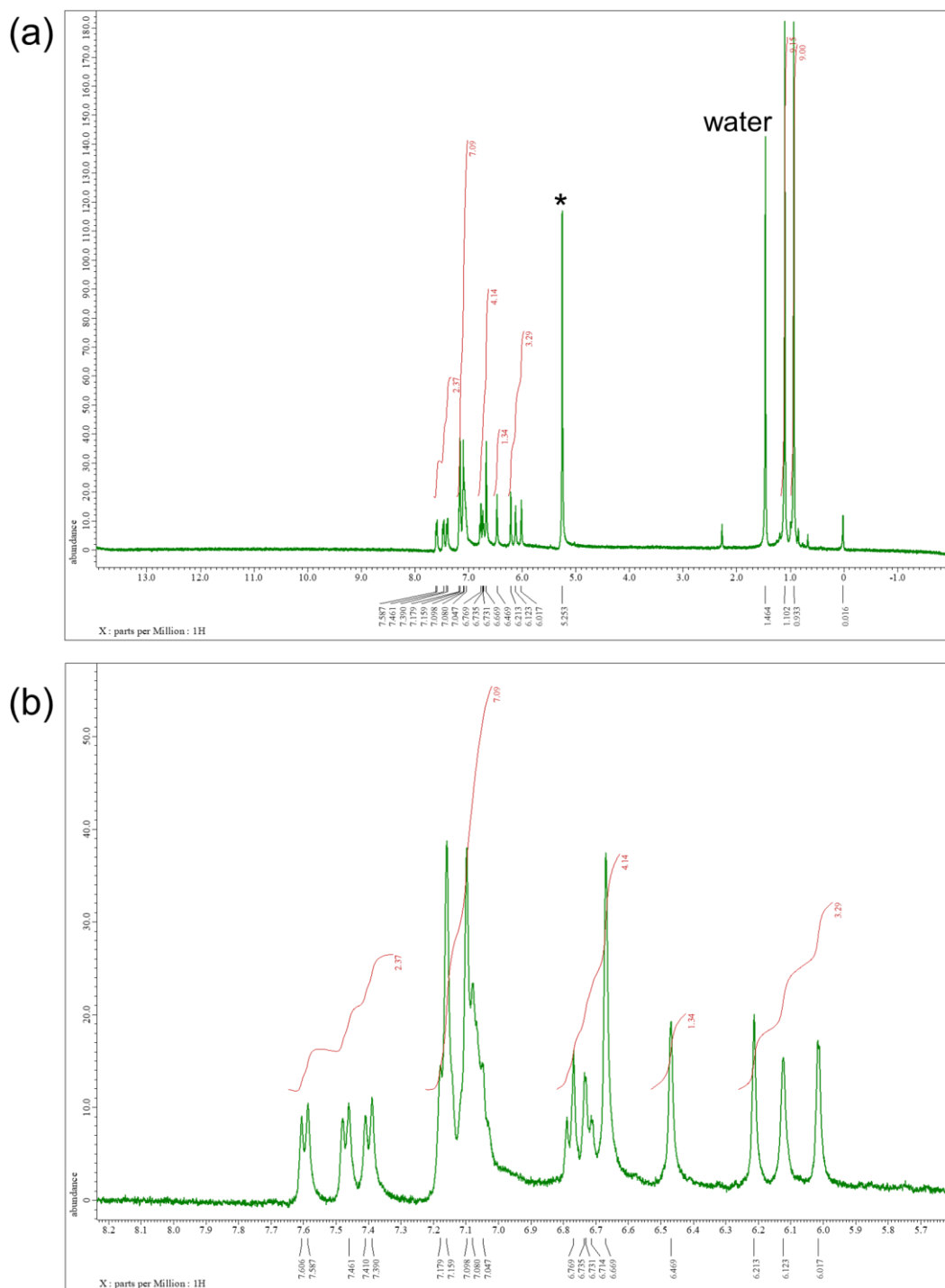


Fig. S2 ^1H NMR spectra of **2** in dichloromethane- d_2 . a) 0–13 ppm and b) aromatic region.

Asterisk denotes the solvent residual peak.

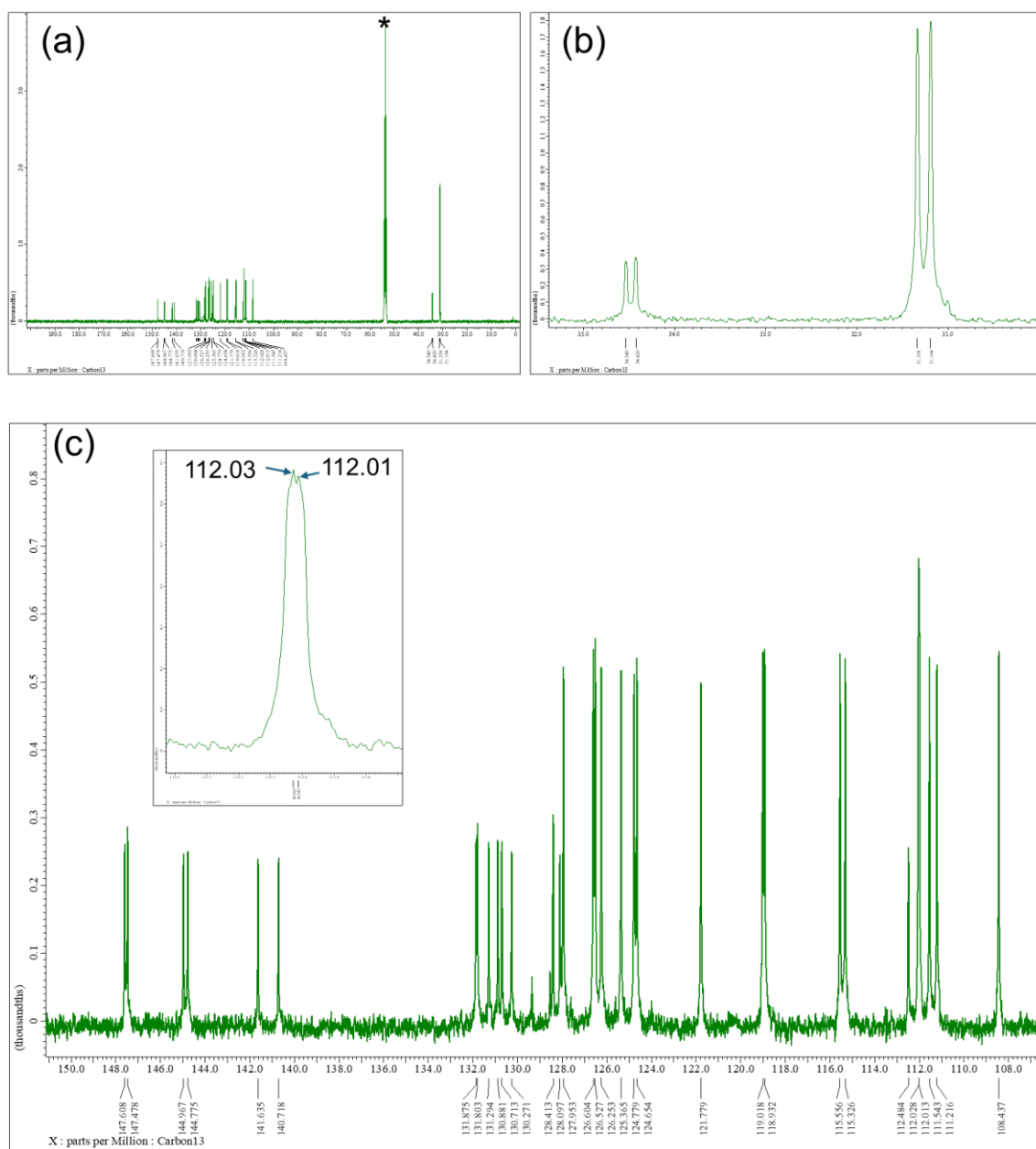


Fig. S3 ^{13}C NMR spectra of **2** in dichloromethane- d_2 . a) 0–200 ppm, b) aliphatic region (30–36 ppm), and c) aromatic region (107–150 ppm). Asterisk denotes the solvent residual peak.

X-ray Crystallography

The single crystals of racemic **2** were obtained by the slow diffusion of methanol into the toluene solution of *rac*-**2**. The single crystals of enantiopure **2** were obtained by slow evaporation of mixed solutions of CH₂Cl₂/hexane. Data collections were performed on a Rigaku Synergy-S diffractometer with Cu-K α radiation at 100 K. The hydrogen atoms were refined using the riding model. All the calculations were performed by using CrystalStructure crystallographic software package,^{S1} except for refinement, which was performed by using SHELXL Version 2017/1.^{S2} The CIF files have been deposited on the Cambridge Crystallographic Data Centre (CCDC), under deposition numbers CCDC 2332276 (*rac*-**2**), 2332277 (*(M)*-**2**) and 2332278 (*(P)*-**2**).

[S1] CrystalStructure 4.3: Crystal Structure Analysis Package, Rigaku Corporation (2000-2018). Tokyo 196-8666, Japan.

[S2] G. M. Sheldrick, *Acta Cryst. A* **2008**, *64*, 112.

Table S1: X-ray crystallographic data for *rac-2* (CCDC 2332276).

empirical formula	C ₄₀ H ₃₆ N ₂ O ₂
formula weight	576.71
<i>T</i> [°C]	−173
λ [Å]	1.54187
crystal system	triclinic
space group	<i>P</i> −1
<i>Z</i>	2
<i>a</i> [Å]	12.0197(7)
<i>b</i> [Å]	12.0255(7)
<i>c</i> [Å]	13.0084(8)
α [°]	87.125(5)
β [°]	64.484(6)
γ [°]	67.794(6)
<i>V</i> [Å ³]	1556.7(2)
ρ_{calcd} [g cm ^{−3}]	1.230
collected data	18901
unique data / <i>R</i> _{int}	6303/0.0352
no. of parameters	397
goodness-of-fit ^[a]	1.042
<i>R</i> 1 (<i>I</i> > 2 σ), <i>wR</i> 2 (all reflections) ^[b]	0.0471, 0.1362
residual density [e Å ^{−3}]	0.23/−0.35

[a] GOF = $\left\{ \sum [w(F_0^2 - F_c^2)^2] / (n - p) \right\}^{1/2}$, where *n* and *p* denote the number of data and parameters.

[b] $R1 = \sum (\|F_0\| - \|F_c\|) / \sum \|F_0\|$ and $wR2 = \left\{ \sum [w(F_0^2 - F_c^2)^2] / \sum [w(F_0^2)^2] \right\}^{1/2}$ where $w = 1 / [\sigma^2(F_0^2) + (a \cdot P)^2 + b \cdot P]$ and $P = [(\text{Max}; 0, F_0^2) + 2 \cdot F_c^2] / 3$.

Table S2: X-ray crystallographic data for (*M*)-**2** (CCDC 2332277).

empirical formula	4(C ₄₀ H ₃₆ N ₂ O ₂) 2(C ₆ H ₁₄)
formula weight	2479.30
<i>T</i> [°C]	−173
λ [Å]	1.54187
crystal system	triclinic
space group	<i>P</i> 1
<i>Z</i>	1
<i>a</i> [Å]	12.3589(2)
<i>b</i> [Å]	12.8347(3)
<i>c</i> [Å]	22.1604(3)
α [°]	79.4229(15)
β [°]	87.2486(13)
γ [°]	87.6565(16)
<i>V</i> [Å ³]	3449.59(11)
ρ_{calcd} [g cm ^{−3}]	1.193
collected data	64819
unique data / <i>R</i> _{int}	22427/0.0523
no. of parameters	1709
goodness-of-fit ^[a]	1.062
<i>R</i> 1 (<i>I</i> > 2 σ), <i>wR</i> 2 (all reflections) ^[b]	0.0518, 0.1470
residual density [e Å ^{−3}]	0.54/−0.25
Flack parameter	0.07(14)

[a] GOF = $\left\{ \sum [w(F_0^2 - F_c^2)^2] / (n - p) \right\}^{1/2}$, where *n* and *p* denote the number of data and parameters.

[b] $R1 = \sum (\|F_0\| - \|F_c\|) / \sum \|F_0\|$ and $wR2 = \left\{ \sum [w(F_0^2 - F_c^2)^2] / \sum [w(F_0^2)^2] \right\}^{1/2}$ where

$w = 1 / [\sigma^2(F_0^2) + (a \cdot P)^2 + b \cdot P]$ and $P = [(\text{Max}; 0, F_0^2) + 2 \cdot F_c^2] / 3$.

Table S3: X-ray crystallographic data for (*P*)-**2** (CCDC 2332278).

empirical formula	4(C ₄₀ H ₃₆ N ₂ O ₂) 2(C ₆ H ₁₄)
formula weight	2479.30
<i>T</i> [°C]	−173
λ [Å]	1.54187
crystal system	triclinic
space group	<i>P</i> 1
<i>Z</i>	1
<i>a</i> [Å]	12.3589(3)
<i>b</i> [Å]	12.8455(3)
<i>c</i> [Å]	22.1587(4)
α [°]	79.4344(17)
β [°]	87.2227(16)
γ [°]	87.6319(19)
<i>V</i> [Å ³]	3452.24(13)
ρ_{calcd} [g cm ^{−3}]	1.192
collected data	65679
unique data / <i>R</i> _{int}	22181/0.0654
no. of parameters	1693
goodness-of-fit ^[a]	1.051
<i>R</i> 1 (<i>I</i> > 2 σ), <i>wR</i> 2 (all reflections) ^[b]	0.0575, 0.1611
residual density [e Å ^{−3}]	0.69/−0.30
Flack parameter	0.14(17)

[a] GOF = $\left\{ \sum [w(F_0^2 - F_c^2)^2] / (n - p) \right\}^{1/2}$, where *n* and *p* denote the number of data and parameters.

[b] $R1 = \sum (\|F_0\| - \|F_c\|) / \sum \|F_0\|$ and $wR2 = \left\{ \sum [w(F_0^2 - F_c^2)^2] / \sum [w(F_0^2)^2] \right\}^{1/2}$ where

$w = 1 / [\sigma^2(F_0^2) + (a \cdot P)^2 + b \cdot P]$ and $P = [(\text{Max}; 0, F_0^2) + 2 \cdot F_c^2] / 3$.

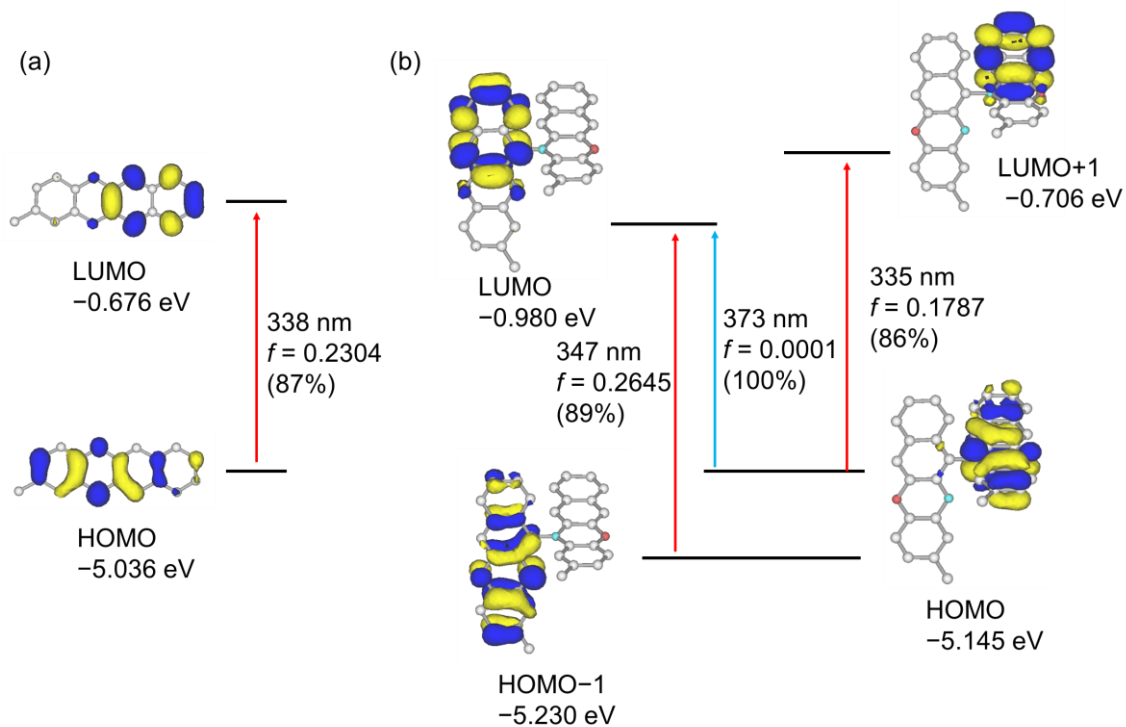


Fig. S4 TD-DFT calculations for (a) 2-methyl benzo[*b*]phenoxazine and (b) **2'** at PBE0/6-31G(d) level of theory.

Table S4. Summary of the results of TD-DFT calculations for the S_1 structure of (*P*)-**2** at the PBE0/6-31G(d) level.

compound ^{a)} (transition)	Energy / nm	$ \mu $ / 10^{-20} esu·cm	$ m $ / 10^{-20} erg·G ⁻¹	$\cos\theta_{\mu,m}$	D / 10^{-40} esu ² ·cm ²	G / 10^{-40} erg ² ·G ⁻²	$R^{b)}$ / 10^{-40} erg·esu· cm·G ⁻¹	f	g_{CPL}
(<i>P</i>)- 2	488	32.8	0.221	0.73	1074	0.0488	5.30	1.0×10^{-3}	2.0×10^{-2}

Table S5. Summary of the results of TD-DFT calculations for the S₁ structure of (*P*)-**2** varying the dihedral angle at the PBE0/6-31G(d) level.

Dihedral angle / °	Energy / nm	$ \boldsymbol{\mu} / 10^{-20}$ esu·cm	$ \boldsymbol{m} / 10^{-20}$ erg·G ⁻¹	$\theta_{\mu,m}$	f	gCPL
60	452	188	0.143	153	3.7×10^{-2}	-2.7×10^{-3}
70	463	154	0.166	157	2.4×10^{-2}	-3.9×10^{-3}
80	474	103	0.183	149	1.0×10^{-2}	-6.2×10^{-3}
90	483	38.2	0.199	136	1.4×10^{-3}	-1.5×10^{-2}
92.5	484	20.9	0.203	128	4.2×10^{-4}	-2.4×10^{-2}
95	486	5.4	0.209	77	2.8×10^{-5}	3.5×10^{-2}
97.5	487	16.8	0.215	34	2.8×10^{-4}	4.3×10^{-2}
99.7 (optimized)	488	32.8	0.221	43	1.0×10^{-3}	2.0×10^{-2}
105	490	72.0	0.240	54	5.0×10^{-3}	7.8×10^{-3}
110	491	109	0.264	63	1.1×10^{-2}	4.5×10^{-3}
120	492	179	0.330	77	3.1×10^{-2}	1.7×10^{-3}

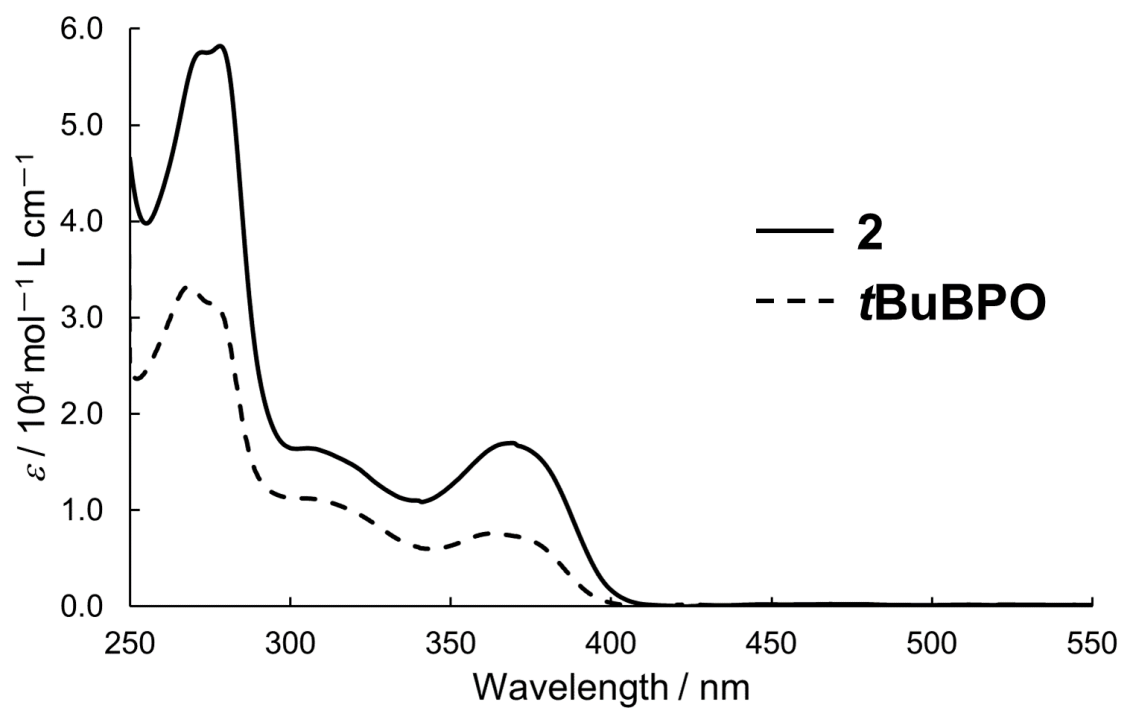


Fig. S5 UV-vis absorption spectra of **2** and *t*BuBPO in dichloromethane at room temperature.

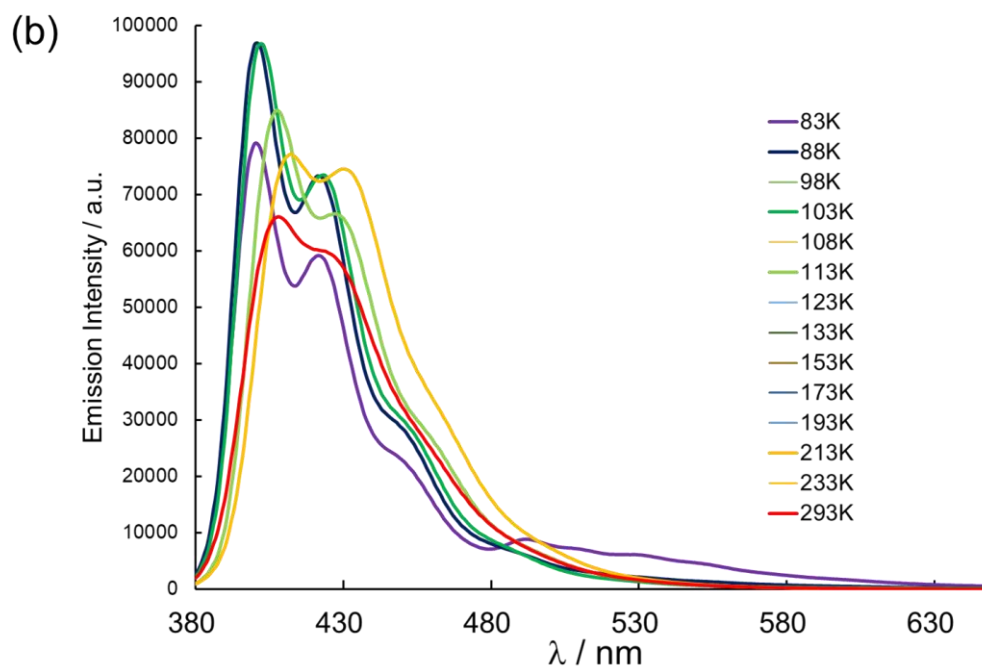
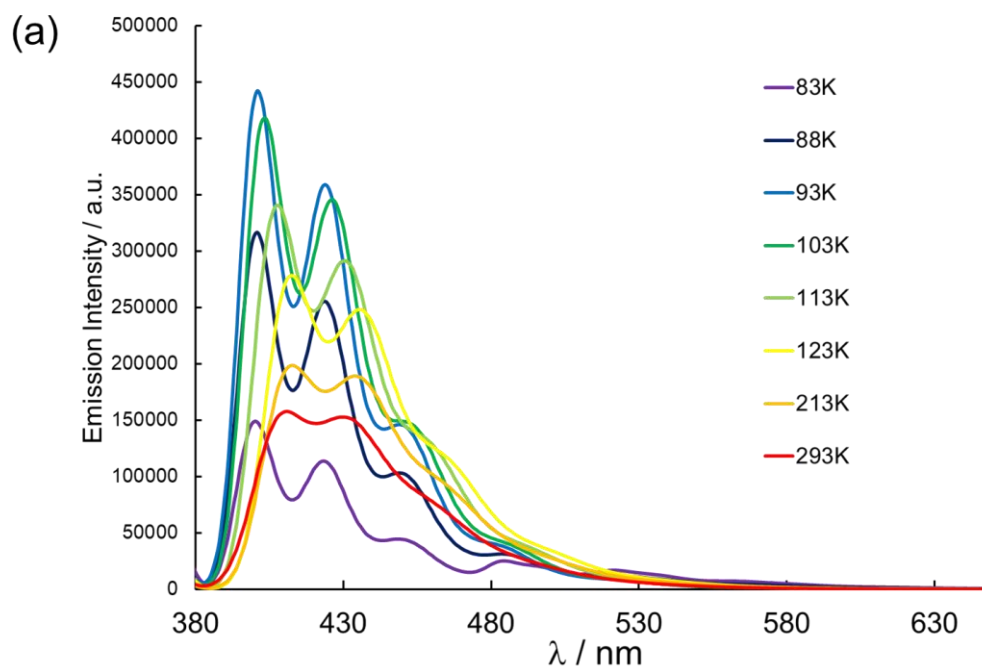


Fig. S6 Temperature dependence of emission spectra of (a) **tBuBPO** and of (b) **2** in 2-MeTHF.

Optical resolution of **2**

Optical resolution of **2** was carried out as follows.

HPLC (JAI LaboACE LC-5060) equipped with a DAICEL CHIRALPAK-IA column (1 cm (i.d.) × 25 cm), eluent: *n*-hexane/2-propanol (95/5, v/v), flow rate: 1.4 mL/min, amount of sample: 0.5 mg)

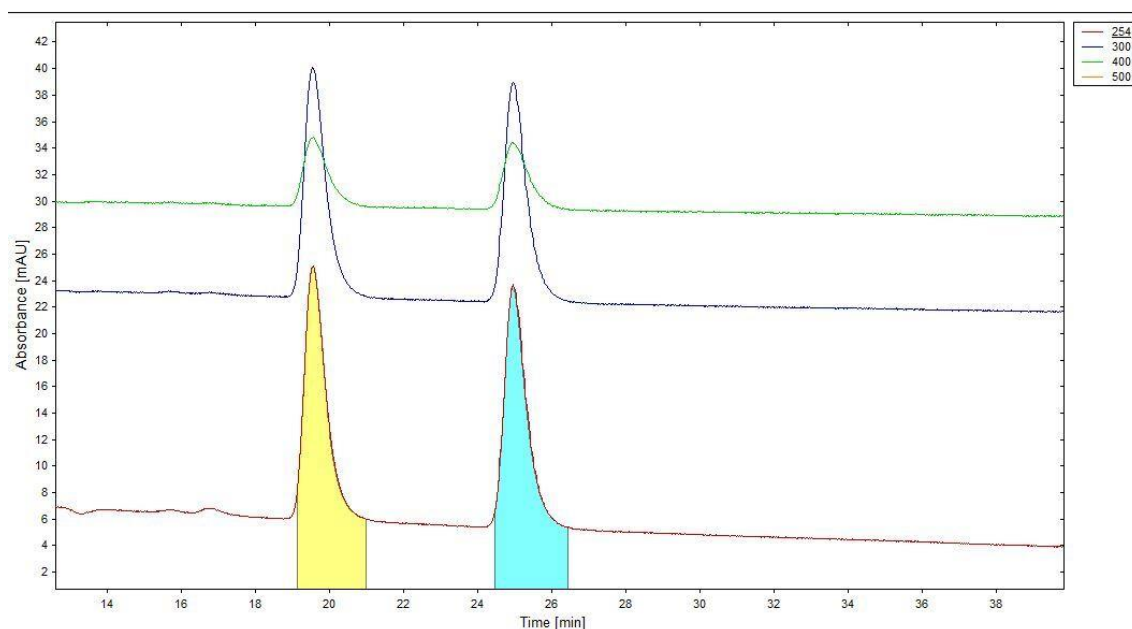


Fig. S7 HPLC chart for the optical resolution of **2**.

Nomenclature of the enantiomers of cruciform dimers

In general, absolute configurations of axially chiral molecules are labeled according to Cahn–Ingold–Prelog priority rules (CIP). However, as described in the main text, the labels of the cruciform dimers of azaacenes based on CIP can be inverted, depending on the substituents on the azaacenes. For example, the CIP labels of each enantiomer of **1** ($R = H$) are inverted if the element of R connected to BPO has an atomic number greater than 6. (Fig. S8a). Therefore, for this class of cruciform dimers of azaacenes, we adopted a nomenclature based on the helicities of double heterohelicenes given by the oxidative ring fusion of the cruciform dimer such that the configuration of the **BPO** skeletons and labeling always correspond, regardless of the substituents (Fig. S8b).

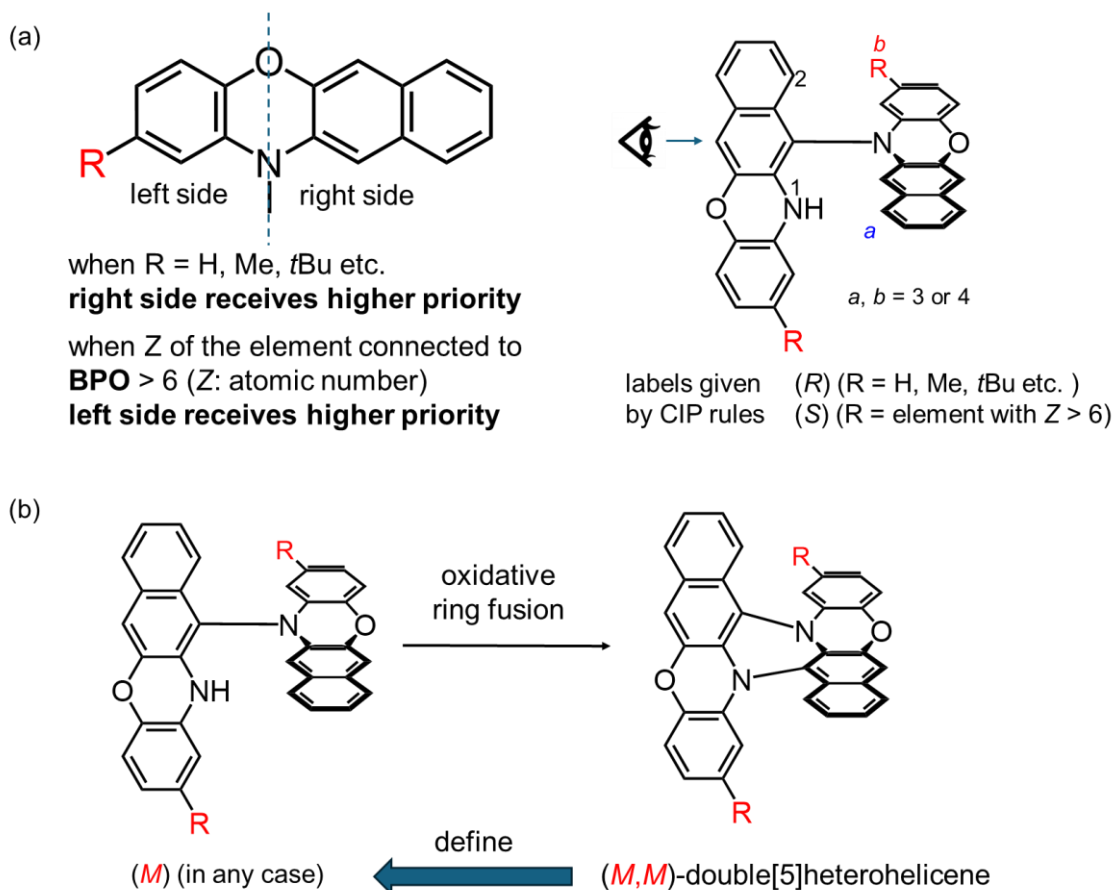


Fig. S8 Nomenclatures of cruciform dimers of azaacenes based on (a) CIP and (b) helicities of double heterohelicenes given by the ring fusion of the cruciform dimer.

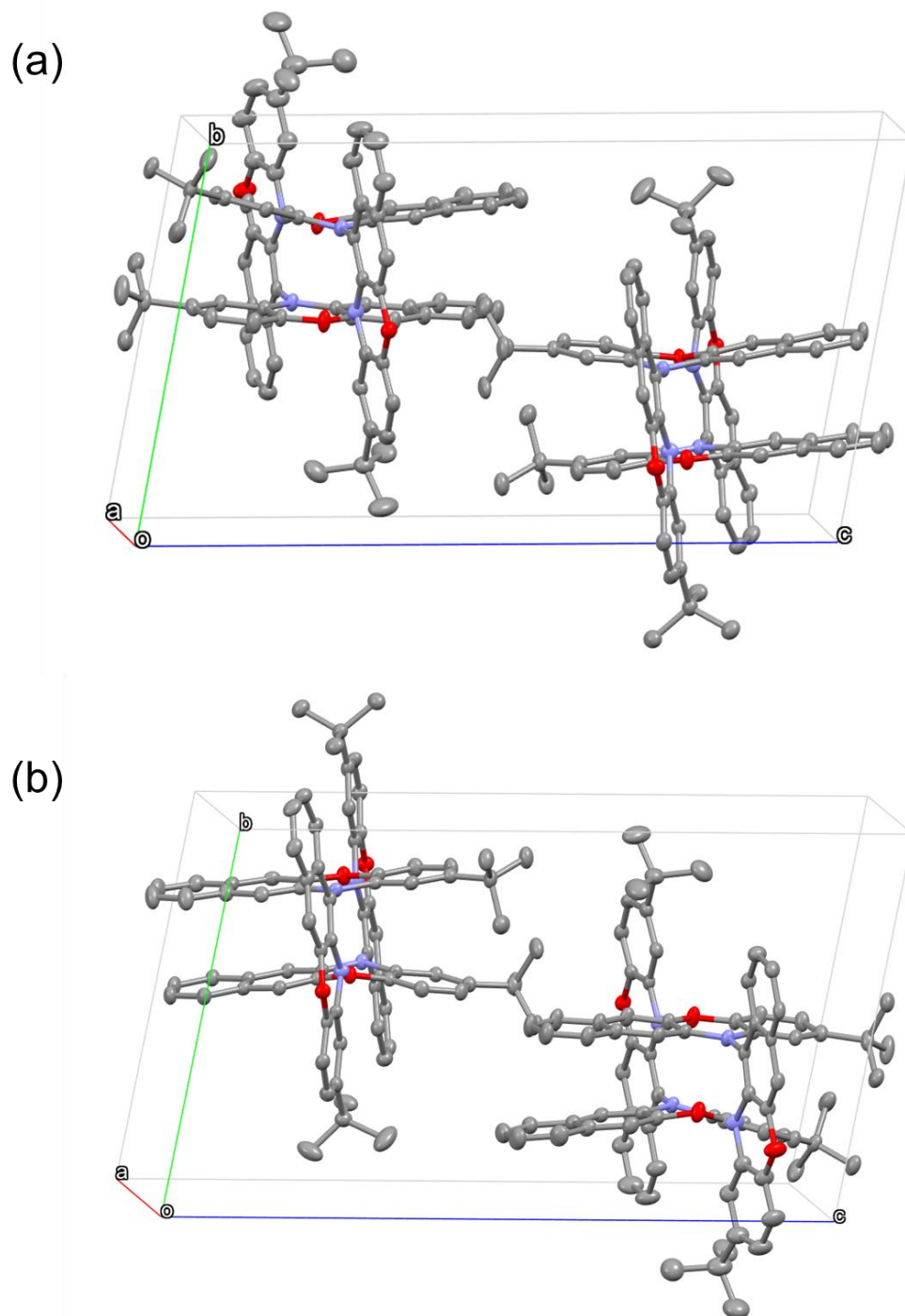


Fig. S9 Packing structures of (a) (*M*)-2 and (b) (*P*)-2.

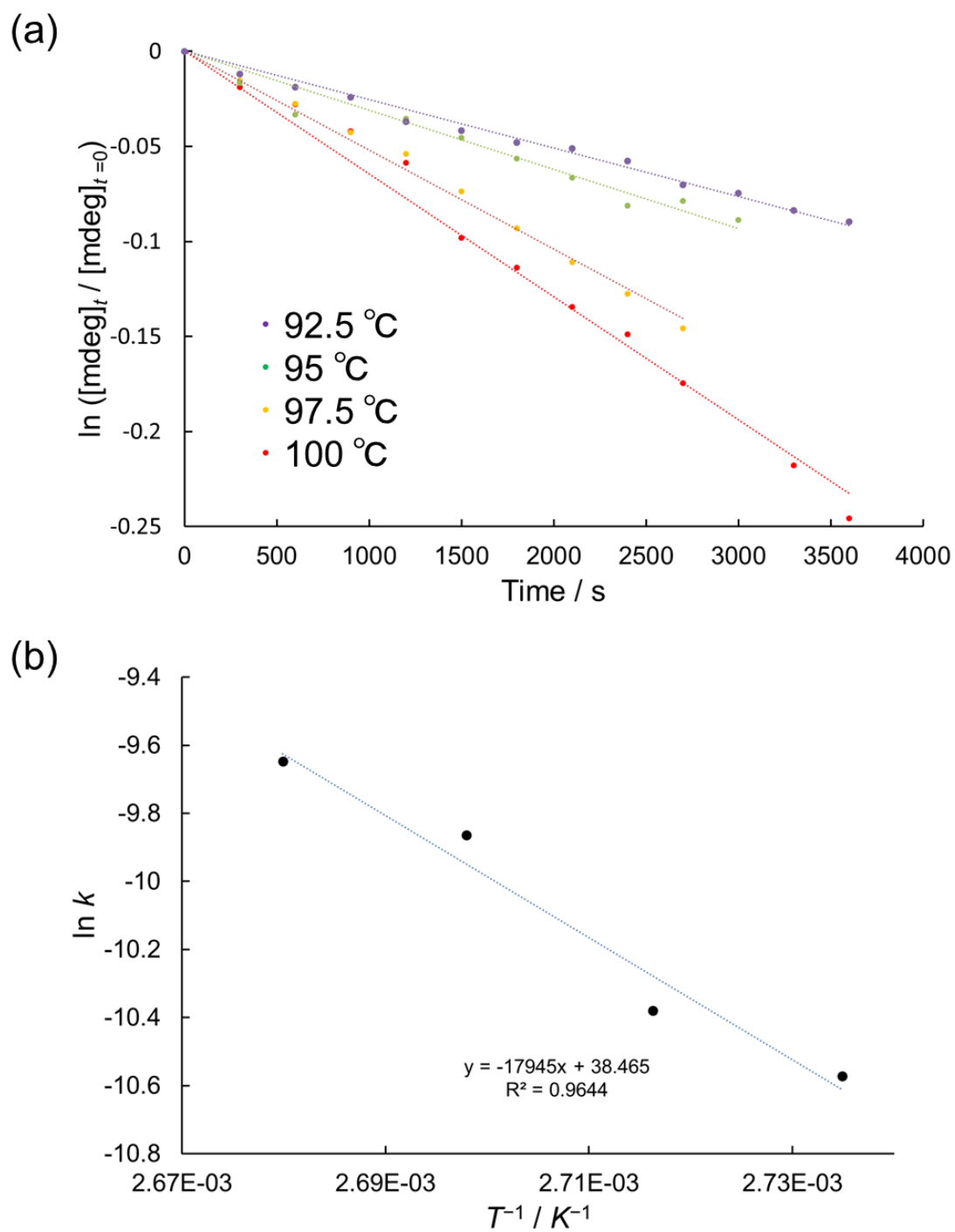


Fig. S10 (a) First order plots of $\ln(\text{CD}/\text{CD}_{t=0})$ of **2** at 380 nm in toluene. (b) Arrhenius plot of k .

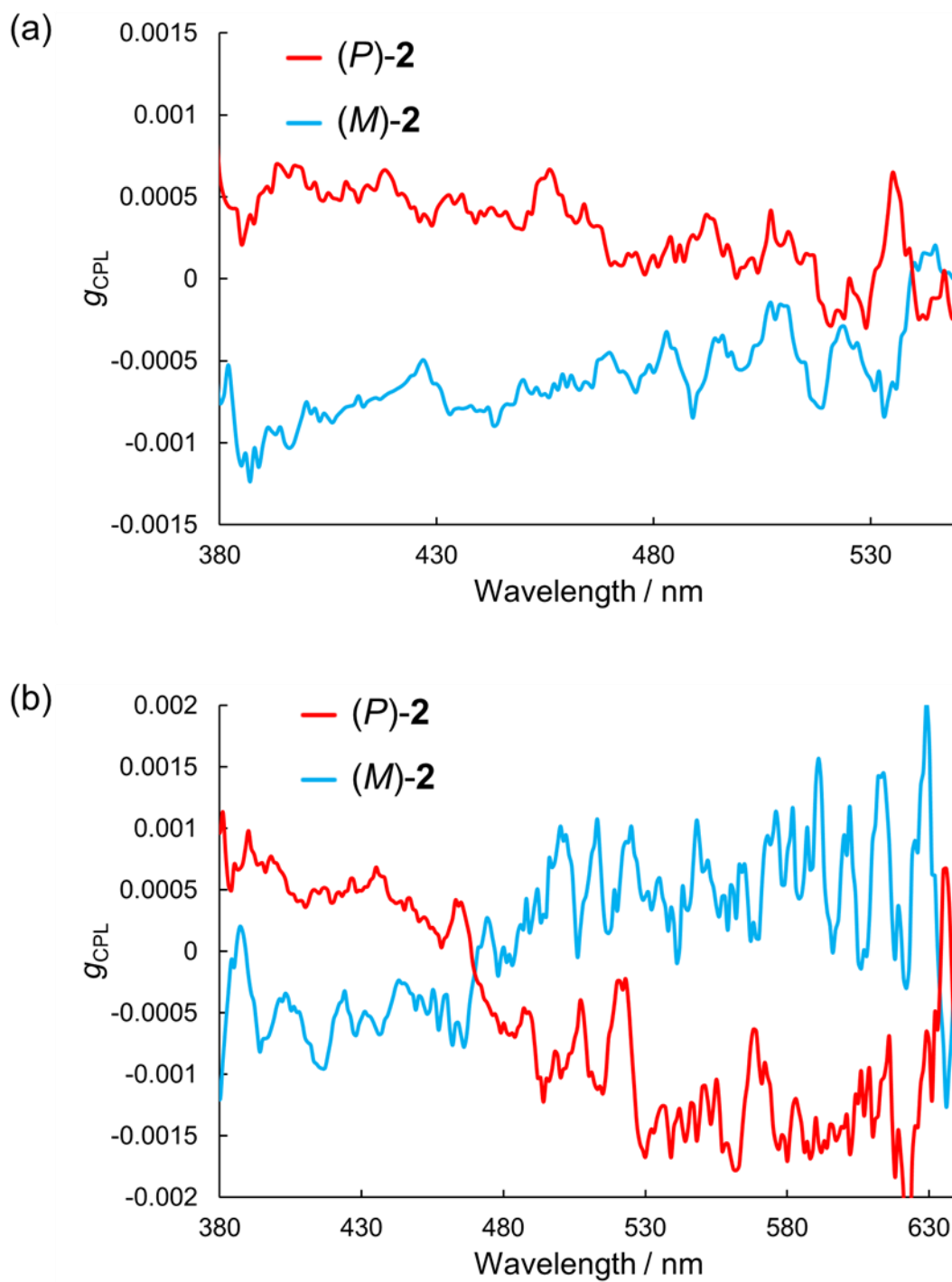


Fig. S11 Plots of g_{CPL} factors versus wavelength of **2** (a) in dichloromethane at 298 K and (b) in 2-MeTHF at 83 K.

Optimized geometry of the S₀ state of (P)-2 calculated at the PBE0/6-31G(d) level of theory

C -4.795920 3.210277 0.609443
H -5.403225 3.297955 1.507466
C -5.015648 4.040445 -0.465457
C -3.779620 2.228666 0.567536
C -2.978876 2.107019 -0.605094
C -4.225027 3.920800 -1.627136
C -3.228592 2.974722 -1.694415
C -3.524392 1.353151 1.652194
C -1.958723 1.123667 -0.647798
H -5.800218 4.790917 -0.421857
H -4.405642 4.579929 -2.471949
H -2.617988 2.880318 -2.589450
H -4.115003 1.415616 2.561736
C -2.530136 0.417933 1.584327
O -2.329032 -0.369810 2.685038
H -1.352357 1.030680 -1.543571
C -1.719996 0.286705 0.417897
N -0.698370 -0.674906 0.416549
C -1.452753 -1.421274 2.590213
C -1.393758 -2.299455 3.656691
C 0.126285 -0.835175 -0.731511
C -0.626042 -1.600540 1.472052
C 0.253346 -2.680494 1.461847
H -2.050434 -2.125025 4.503556
C -0.504229 -3.371945 3.632684
H -0.464359 -4.053417 4.478187
H 0.892346 -2.824303 0.595335
C 0.327717 -3.575487 2.534928
C 1.286695 -4.732609 2.481355
C 1.331871 -0.158041 -0.754279
C -0.275782 -1.666655 -1.818699
C 0.596335 -1.788831 -2.940052
C 2.189808 -0.296580 -1.885446
C 1.830364 -1.084727 -2.939025
C -1.500587 -2.370353 -1.822710
C 0.209582 -2.609411 -4.022307
N 1.740571 0.647913 0.277581
O 3.390761 0.355956 -1.939462
H 2.507454 -1.167457 -3.784185
H -2.164857 -2.277328 -0.968970
C -1.848767 -3.162785 -2.893963
H -2.794660 -3.697268 -2.882918
H 0.879082 -2.698463 -4.874695
C -0.989686 -3.284951 -4.002841

H	-1.275142	-3.912636	-4.842336
H	1.128707	0.744673	1.073767
C	2.957244	1.310652	0.245958
C	3.394933	2.123819	1.285446
C	3.773323	1.147613	-0.881358
C	4.996248	1.785671	-0.955816
H	2.757542	2.247677	2.159203
C	4.630110	2.778684	1.225478
C	5.072909	3.659567	2.360682
H	5.606095	1.637804	-1.841701
C	5.423341	2.598425	0.094694
H	6.386973	3.095603	0.026083
H	1.035038	-5.422011	1.666411
H	2.315248	-4.393862	2.310343
H	1.273034	-5.302225	3.415329
H	4.416650	4.531649	2.469376
H	5.056370	3.121916	3.315893
H	6.090645	4.028030	2.202310

Optimized geometry of the S₁ state of (*P*)-2 calculated at the PBE0/6-31G(d) level of theory

C	-5.043961	-2.953882	-0.385481
H	-5.621068	-3.126794	-1.290020
C	-5.352750	-3.613973	0.777274
C	-3.968423	-2.033912	-0.424829
C	-3.203970	-1.805340	0.768405
C	-4.603733	-3.386954	1.958564
C	-3.556433	-2.504918	1.955349
C	-3.628003	-1.330145	-1.599304
C	-2.130053	-0.903030	0.745481
H	-6.180453	-4.317071	0.796796
H	-4.866477	-3.917081	2.869058
H	-2.978007	-2.323222	2.856694
H	-4.189044	-1.475136	-2.517309
C	-2.580835	-0.448505	-1.592775
O	-2.295113	0.208725	-2.749880
H	-1.545375	-0.704453	1.636904
C	-1.796765	-0.223211	-0.418938
N	-0.734450	0.655619	-0.465790
C	-1.281133	1.099249	-2.772252
C	-1.040039	1.770711	-3.965353
C	0.085501	0.877291	0.699832
C	-0.483116	1.341638	-1.626541
C	0.559972	2.282504	-1.718049
H	-1.670906	1.557376	-4.821670
C	-0.009967	2.689063	-4.023134

H	0.179889	3.216874	-4.953689
H	1.157779	2.456158	-0.831703
C	0.803428	2.958577	-2.896603
C	1.910784	3.965719	-2.997870
C	1.327859	0.188344	0.765908
C	-0.300139	1.893911	1.623235
C	0.641878	2.205852	2.670967
C	2.198989	0.534775	1.778752
C	1.884522	1.522660	2.713213
C	-1.516249	2.598764	1.567589
C	0.290847	3.202497	3.604677
N	1.667054	-0.786862	-0.200862
O	3.439675	-0.071398	1.907992
H	2.610917	1.758925	3.483607
H	-2.231183	2.381793	0.778279
C	-1.825757	3.585691	2.514372
H	-2.773925	4.112763	2.446972
H	1.002042	3.441339	4.392062
C	-0.926670	3.882503	3.528459
H	-1.163824	4.646248	4.264942
H	0.908732	-1.420616	-0.427290
C	2.883723	-1.460100	-0.005137
C	3.266052	-2.506814	-0.839091
C	3.744442	-1.073460	1.034615
C	4.956016	-1.726701	1.203325
H	2.594201	-2.794962	-1.646863
C	4.478640	-3.182496	-0.672333
C	4.852938	-4.313341	-1.590976
H	5.598766	-1.409105	2.018981
C	5.321627	-2.772518	0.358405
H	6.273779	-3.274658	0.510523
H	1.518513	4.952572	-3.269634
H	2.448772	4.062974	-2.052391
H	2.631478	3.677968	-3.772087
H	4.127739	-5.134792	-1.536915
H	4.892527	-3.987550	-2.637697
H	5.835059	-4.722155	-1.334426